Article

Facile Synthesis of CuO Nanocrystals with Systematic Shape Evolution from Cubic to Octahedral Structures

Chun-Hong Kuo, and Michael H. Huang

J. Phys. Chem. C, **2008**, 112 (47), 18355-18360 • Publication Date (Web): 31 October 2008

Facile Synthesis of Cu_2O Nanocrystals with Systematic Shape Evolution from Cubic to Octahedral Structures

Chun-Hong Kuo and Michael H. Huang*

Department of Chemistry, National Tsing Hua University, Hsinchu 30013, Taiwan

Received: July 8, 2008; Revised Manuscript Received: August 20, 2008

We report a facile method for the synthesis of cuprous oxide nanocrystals with systematic shape evolution. Monodisperse truncated cubic, cuboctahedral, truncated octahedral, and octahedral nanocrystals can be synthesized directly in an aqueous solution of $CuCl_2$, sodium dodecyl sulfate (SDS) surfactant, hydroxylamine ($NH_2OH \cdot HCl$) reductant, and NaOH by simply varying the volume of hydroxylamine added to the reaction mixture. SDS surfactant was found to be necessary for a precise control of the nanocrystal morphology. Adjustment of the volume of NaOH added provides a means to vary the particle size. In the case of octahedral nanocrystals, particles with sizes of 160−460 nm can be prepared. By examining the intermediate products formed, which resemble the final nanocrystal structures, a growth mechanism is proposed. Optical characterization of these Cu_2O nanocrystals showed band gap absorption at 470−490 nm and strong light scattering bands extending from the visible to the near-infrared light region. All four samples displayed activity toward photodegradation of rhodamine B molecules, but truncated octahedral and octahedral nanocrystals exhibited a higher extent of the photodecomposition reaction, suggesting the {111} faces of Cu_2O nanostructures are catalytically more active than the {100} faces. These nanocrystals should allow the examination of their various properties as a function of the particle shape.

Introduction

Cuprous oxide (Cu_2O) is a p-type semiconductor with a direct band gap of 2.17 eV.[1] Cu_2O nanostructures have been demonstrated to be useful for gas sensing,[2,3] photodegradation of dye molecules,[4] CO oxidation,[5] photoactivated water splitting into H_2 and O_2,[6] and organic synthesis.[7] A variety of Cu_2O nanostructures such as nanoplates,[1] nanocubes,[8−14] octahedra,[4,12−14] spherical particles,[14] nanocages,[15−20] nanowires,[21−23] and other highly symmetrical structures have been synthesized in recent years.[24,25] Among these morphologies, Cu_2O nanocrystals with cubic and octahedral geometries are perhaps the most interesting, because other more complex particle structures can be derived from these simple structural forms, and their well-defined surfaces provide unique opportunities for the examination of their facet-specific properties. Procedures available describing the formation of cubic and octahedral Cu_2O nanocrystals and their intermediate structures in a single system are mainly limited to a cathodic deposition method with crystals growing directly on the electrode surface.[12−14] The experimental setup seems costly with precious metal-coated electrode surfaces, and an effective removal of these Cu_2O crystals from the substrates may present a problem. A simple and inexpensive procedure which can form monodisperse Cu_2O nanocrystals with these structures directly in an aqueous solution should be highly desirable for their subsequent property characterization and potential applications.

In this study we have developed a facile and low-cost aqueous colloidal solution approach for the syntheses of monodisperse Cu_2O truncated nanocubes, cuboctahedra, truncated octahedra, and octahedra at room temperature. The systematic variation in the product morphology can be controlled by changing the amount of reductant added. A detailed crystal structure analysis has been performed on these Cu_2O nanocrystals. On the basis of the intermediate particles obtained during the nanocrystal formation process, a growth mechanism is proposed. We have also considered the effect of a capping surfactant on the formation of these structurally well-defined Cu_2O nanoparticles. The sizes of these nanocrystals can be tuned to some degree by controlling the volume of sodium hydroxide added to the reaction mixture. Optical absorption spectra of these Cu_2O nanocrystals were taken to see how the particle shape and size affect their absorption characteristics. The ability to prepare these nanocrystals with distinct structures allows us to compare their photocatalytic activity toward the decomposition of rhodamine B. Such an experiment reveals how crystal faces can affect the catalytic activity of these Cu_2O nanocrystals.

Experimental Section

Anhydrous copper(II) chloride ($CuCl_2$; 97%) and hydroxylamine hydrochloride ($NH_2OH \cdot HCl$; 99%) were purchased from Aldrich. Sodium hydroxide (NaOH; 98.2%) and sodium dedecyl sulfate (SDS; 100%) were acquired from Mallinckrodt. All chemicals were used without further purification. For the syntheses of Cu_2O nanocrystals with different product morphologies, 9.4, 9.2, 9.0, and 8.8 mL of deionized water (18.3 MΩ) were respectively added to four sample bottles labeled A, B, C, and D. Then 0.1 mL of 0.1 M $CuCl_2$ solution and 0.087 g of SDS powder were added to each bottle with vigorous stirring until dissolution of the powder, and the resulting solutions were allowed to stand for 5 min. Next, 0.25, 0.45, 0.65, and 0.85 mL of 0.2 M $NH_2OH \cdot HCl$ were mixed with the solutions in bottles A, B, C, and D, respectively. After the solutions were shaken for 10 s, 0.25 mL of 1.0 M NaOH was added, and the bottles were shaken for an additional 10 s. The total solution volume in each bottle is 10 mL, and the respective concentrations of Cu^{2+} ions and SDS surfactant in the final

* To whom correspondence should be addressed. E-mail: hyhuang@mx.nthu.edu.tw.

10.1021/jp8060027 CCC: $40.75
Published on Web 10/31/2008

SCHEME 1: Schematic Illustration of the Procedure Used To Grow Cu_2O Nanocrystals of Different Shapes

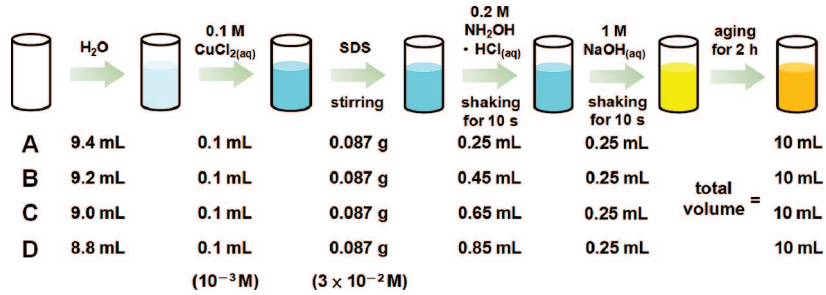

solution are 10^{-3} and 3×10^{-2} M. The solution color turned from light blue to yellow within seconds after the addition of NaOH. We aged the solutions for 2 h to obtain the desired Cu_2O nanocrystal products. A schematic diagram of the preparation procedure is given in Scheme 1. After aging, the four samples were centrifuged at 5000 rpm for 5 min (Hermle Z323 centrifuge). The precipitates were centrifuged twice more in ethanol to remove unreacted chemicals and the SDS surfactant and finally dispersed in 0.5 mL of ethanol. A drop of the precipitate solution was transferred to either a carbon-coated copper grid or a clean silicon wafer for electron microscopy observation.

For the examination of the photocatalytic activity of these Cu_2O nanocrystals, each of the four samples was similarly centrifuged three times, and finally, the entire precipitate was dispersed in 20 mL of 2.5 mg/L aqueous rhodamine B solution. Then 3 mL of this solution was transferred to a standard quartz cell. The cell was irradiated with light from a 100 W mercury lamp placed 20 cm away. The solution was constantly stirred during photoirradiation. UV−vis absorption spectra of these samples were taken before and after every 60 min of irradiation for up to 360 min.

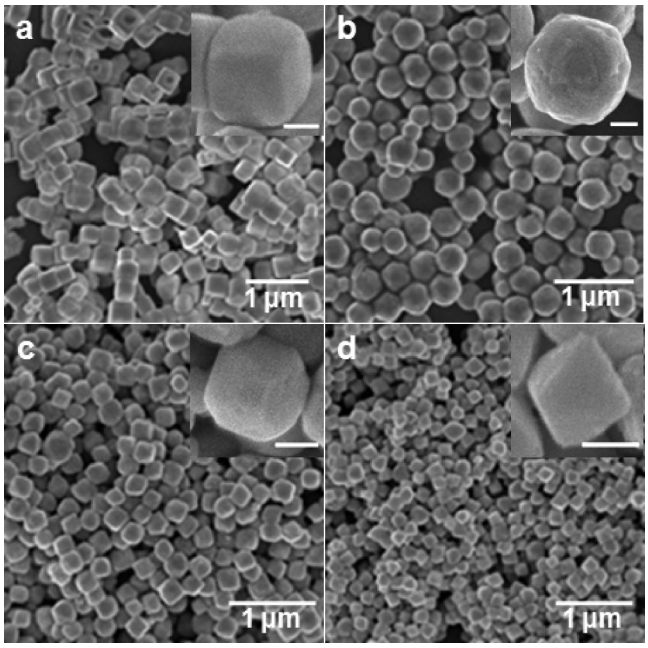

Figure 1. (a−d) Respective SEM images of the Cu_2O nanocrystals synthesized in sample bottles A, B, C, and D with increasing amounts of $NH_2OH \cdot HCl$ added to the solutions in the bottles. The particle morphologies are (a) truncated cubic, (b) cuboctahedral, (c) truncated octahedral, and (d) octahedral in shape. Insets show the enlarged views of individual nanocrystals. The scale bar in the inset is equal to 100 nm.

TABLE 1: Average Particle Sizes and Standard Deviations of the Cu_2O Nanocrystals Synthesized in Samples A−D

sample	morphology	av particle size (nm)	std dev (%)
A	truncated cubic	296 ± 39	13
B	cuboctahedral	382 ± 27	7
C	truncated octahedral	218 ± 25	11
D	octahedral	162 ± 20	12

Scanning electron microscopy (SEM) images of the synthesized Cu_2O nanocrystals were obtained using JEOL JSM-7000F and JSM-7401F scanning electron microscopes. Transmission electron microscopy (TEM) characterization was performed on a JEOL JEM-2000FX electron microscope operating at 160 kV and a JEM-2010 electron microscope operating at 200 kV. Powder X-ray diffraction (XRD) patterns were collected using a Shimadzu XRD-6000 diffractometer with Cu Kα radiation ($\lambda = 1.5418$ Å). UV−vis absorption spectra were acquired using a JASCO V-570 spectrophotometer.

Results and Discussion

In this study, the syntheses of Cu_2O nanocrystals with systematic shape evolution from cubic to octahedral structures was achieved by simply varying the amount of reductant $NH_2OH \cdot HCl$ added to the reaction mixture. It is expected that $Cu(OH)_4^{2-}$ ions form readily upon the addition of NaOH and are reduced to Cu_2O by NH_2OH in the following reaction:

$$2Cu(OH)_4^{2-} + 2NH_2OH \rightarrow Cu_2O + N_2 + 5H_2O + 4OH^-$$

The growth process will be described later. However, the above reaction suggests that the formation of different Cu_2O nanostructures may be related to the concentration of hydroxide ions in the solution. Figure 1 shows the SEM images of the Cu_2O nanocrystals synthesized in sample bottles A−D. Different particle morphologies can be clearly distinguished in these samples, especially with the help of the magnified images of individual particles. These nanocrystals exhibit truncated cubic, cuboctahedral, truncated octahedral, and octahedral structures. The nanocubes produced in sample bottle A have truncated corners and edges as described in our previous study on the seed-mediated synthesis of Cu_2O nanocubes.[8] Here the cuboctahedral nanocrystals refer to particles composed of six square {100} faces and eight truncated triangular or hexagonal {111} faces, as both products were observed in sample bottle B. Truncated octahedral nanocrystals are those with an octahedral structure bound by {111} faces but with flat {100} corners. Table 1 lists the average particle sizes and standard deviations for the four samples obtained from their size distribution histograms (see the Supporting Information). Interestingly, the nanocrystals in each sample are highly monodisperse in size with a small standard deviation of 13% or less. No other product morphologies were observed in these SEM images, demonstrat-

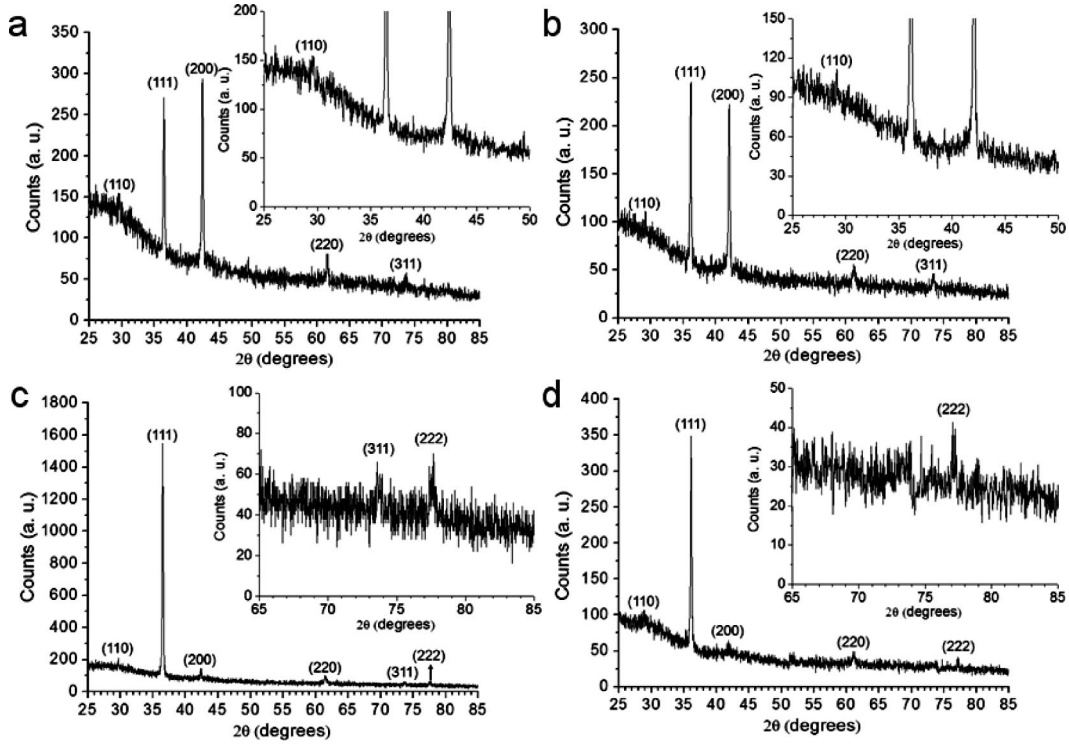

Figure 2. XRD patterns of the synthesized Cu_2O nanocrystals with (a) truncated cubic, (b) cuboctahedral, (c) truncated octahedral, and (d) octahedral structures. The insets show the enlarged patterns for selected 2θ ranges. Note the variation in the ratio of the intensity of the (200) peak to that of the (111) peak.

ing the effective and high-yield growth of highly monodisperse Cu_2O nanocrystals with systematic shape evolution using the current synthesis approach.

The identity and detailed crystal structure of these nanocrystals were verified with XRD and TEM characterization. Figure 2 gives the XRD patterns for the four samples. The XRD patterns show the expected (110), (111), (200), (220), (311), and (222) reflection peaks of Cu_2O and confirm that these nanocrystals have a cubic crystal structure of Cu_2O (a body-centered cubic packing of oxygen atoms with copper atoms occupying half of the tetrahedral sites). The ratios of the intensity of the (200) peak to that of the (111) peak are progressively lowered from truncated cubic to octahedral nanocrystals as a result of the decreasing {100} faces. A similar trend has been observed for gold cubes to octahedra.[26] This change in the intensity ratio also results from the preferential deposition of nanocubes on their {100} faces and octahedra on their {111} faces. Other than this general trend, it is worthy to note that the intensity of the (200) peak is comparable to that of the (111) peak for the truncated cubic and cuboctahedral nanocrystals. A drastic decrease in the intensity of the (200) peak relative to the (111) peak was observed for both the octahedral and truncated octahedral nanocrystals. Figure 3 presents the TEM images and corresponding selected-area electron diffraction (SAED) patterns of two cuboctahedral Cu_2O nanocrystals viewed along the [111] and [001] directions and those of a truncated octahedron viewed along the [111] direction. The TEM results further confirm their morphologies observed in the SEM images. Schematic drawings of these nanocrystals with labeled facets are provided to help visualize the orientations of these particles.

The formation process of these Cu_2O nanocrystals with systematic shape evolution was examined by observing the intermediate structures formed. Figure 4 displays intermediate Cu_2O nanocrystals obtained from sample bottles A, B, and D after the final solutions were aged for just 5 min. Nanoparticles with rough surfaces but overall cubic, cuboctahedral, and octahedral morphologies have already appeared, indicating a rapid crystal growth has occurred. These intermediate structures seem to be formed through the aggregation of smaller crystals 50−100 nm in diameter. Simultaneously, tiny Cu_2O nanoparticles 10−20 nm in diameter adsorbing on the surfaces of these intermediate structures and disordered nanoparticle aggregates next to octahedral nanocrystals were observed (see the Supporting Information). These small nanoparticles may be in the process of growing over an existing intermediate structure or forming a new intermediate structure. From the results of this investigation, a growth mechanism of these Cu_2O nanocrystals is proposed and shown in Scheme 2. Immediately after the addition of $NH_2OH\cdot HCl$ and NaOH, small Cu_2O seed particles are formed, as evidenced by an instant change of the solution color. These seed particles quickly aggregate into larger particles tens of nanometers in size. The aggregation process continues, forming the observed intermediate structures in 5 min with sizes approaching the final nanocrystal dimensions. For some particle aggregates, intermediate structures resembling the final products have yet to form. Seed particles continuously adsorb onto these intermediate structures to allow further growth through a ripening process. The capping surfactant SDS and the amount of $NH_2OH\cdot HCl$ present in the solution play a crucial role in directing the overall morphology of these intermediate structures. The amount of $NH_2OH\cdot HCl$ may influence the growth rate along the [100] direction relative to that of the [111] direction, or the value of R, and results in the formation of intermediate structures with roughly cubic, cuboctahedral, and octahedral structures. For example, when R is 1.15 and 1.73, truncated octahedral and perfect octahedral particles are produced.[27] The intermediate structures then develop into structurally well-defined final products via a surface reconstruction process in 2 h. It is interesting to note how small differences in the amount

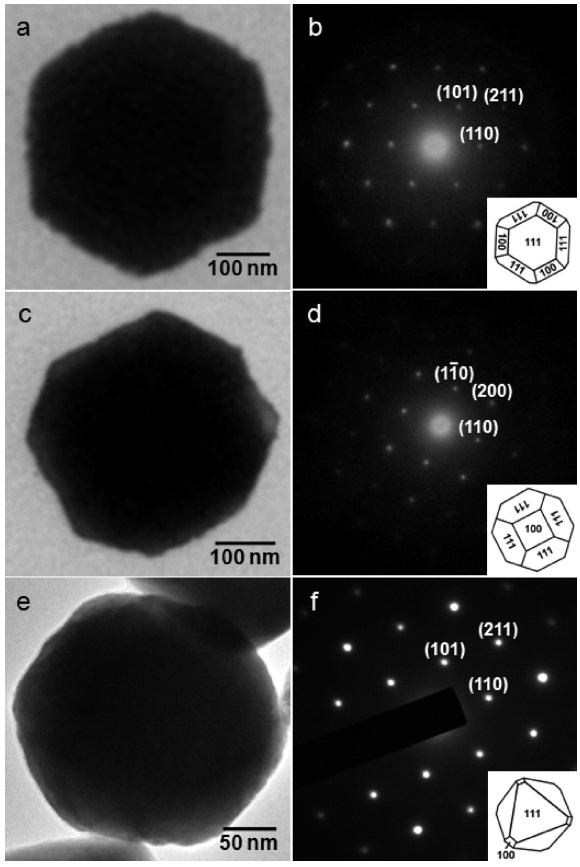

Figure 3. (a, b) TEM image of a cuboctahedron viewed along the [111] direction and its corresponding SAED pattern recorded along the [1$\bar{1}\bar{1}$] zone axis. (c, d) TEM image of another cuboctahedron viewed along the [001] direction and its corresponding SAED pattern recorded along the [00$\bar{1}$] zone axis. (e, f) TEM image of a truncated octahedron viewed along the [111] direction and its corresponding SAED pattern recorded along the [1$\bar{1}\bar{1}$] zone axis. The insets show the orientations of these nanocrystals with labeled facets. The cuboctahedral particles were obtained from sample B, and the truncated octahedron was from sample C.

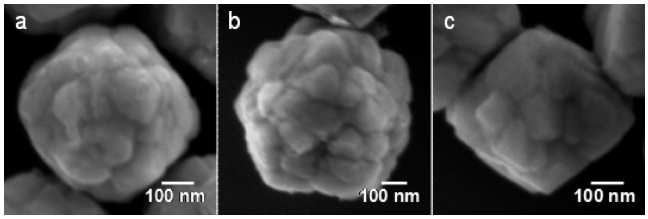

Figure 4. (a−c) SEM images of intermediate Cu_2O nanocrystals obtained from sample bottles A, B, and D after the final solutions were aged for just 5 min. Interestingly, these particles show morphologies resembling that of a cube, a cuboctahedron, and an octahedron. The irregular surface structure of these particles suggests the formation of the final products via the aggregation of individual smaller particles and the surface reconstruction process.

of the reductant $NH_2OH \cdot HCl$ added to the four solutions can exert such a profound effect on the nanocrystal morphology. The addition of NaOH made all the solutions basic. A larger amount of $NH_2OH \cdot HCl$ added indeed made the solution slightly less basic from a pH of 12.05 for sample A to 11.34 for sample D with HCl from $NH_2OH \cdot HCl$ reacting with NaOH. However, octahedral nanocrystals can also be synthesized at a pH used to grow truncated cubic particles (see the discussion below and the Supporting Information). This analysis suggests that the amount of NH_2OH added to the solution, rather than small changes in the solution pH, is mainly responsible for the shape control of Cu_2O nanocrystals synthesized in this system. The role of SDS in assisting the cubic and octahedral nanocrystal formation was verified by replacing SDS with the same mole number of cetyltrimethylammonium bromide (CTAB) surfactant. SEM characterization of the Cu_2O products prepared in the four solutions revealed only the formation of quasi-spherical particles largely 100−200 nm in diameter through particle aggregation (see the Supporting Information), demonstrating the choice of capping surfactant used is also very important for the effective shape-controlled synthesis of these Cu_2O nanocrystals.

The sizes of these cuprous oxide nanocrystals can be varied to some degree by simply adjusting the volume of NaOH added to the solutions. Figure 5 provides the SEM images of the Cu_2O nanocrystals formed in samples A−D by increasing the volume of 1.0 M NaOH added to the reaction mixture to 0.75 mL. The particle morphologies remain the same as before, but their dimensions have increased considerably. The largest size increase was recorded for the octahedral nanocrystals from an average size of 162 nm (with 0.25 mL of NaOH added) to an average size of 429 nm. Particle size distributions for all the conditions (that is, 0.250, 0.375, 0.500, 0.625, and 0.750 mL of NaOH added) are also narrow with standard deviations of 15% or less (see the Supporting Information for the solution pH values, particle sizes, and their standard deviations with the addition of 0.25−0.75 mL of 1.0 M NaOH). Again the pH values of the solutions in samples A−D varied only slightly with different volumes of NaOH added (less than a pH change of 1).

The optical properties of these Cu_2O nanocrystals were examined by UV−vis absorption spectroscopy. Figure 6 gives the UV−vis absorption spectra for samples A−D prepared using the procedure shown in Scheme 1 with the addition of 0.25 mL of 1.0 M NaOH. Except for samples A and B showing a weak absorption band in the 450−480 nm range, absorption spectra for all the samples are dominated by strong light scattering bands resulting from the relatively large sizes of these nanocrystals.[8] The positions of these single or multiple light scattering bands display a progressive blue shift from the near-infrared (NIR) region for samples A and B with nanocrystals of 300−380 nm in size to the visible light region for samples C and D with particle sizes of 160−220 nm. A well-resolved absorption band has been recorded from samples prepared with the addition of 0.75 mL of 1.0 M NaOH, because the edge of the light scattering band is more widely separated from the absorption band for these larger Cu_2O nanocrystals with particle sizes of 430−570 nm (see the Supporting Information). These nanocrystals absorb at 470−490 nm, and their calculated band gap energy is in the range of 2.53−2.64 eV. This greater band gap value, as compared to that of bulk Cu_2O at 2.17 eV, is attributed to quantum confinement effects. Interestingly, this value is somewhat larger than that previously found for Cu_2O nanocubes of smaller sizes.[8]

The ability to synthesize Cu_2O nanocrystals with this systematic shape evolution provides a unique opportunity to examine their relative photocatalytic activity toward the degradation of dye molecules. Figure 7 is a plot of the extent of photodecomposition of rhodamine B as a function of the irradiation time for the blank and the four samples prepared with the addition of 0.75 mL of 1.0 M NaOH. All the synthesized particles in each sample were collected and used for this photodecomposition study. These samples with larger Cu_2O nanocrystals were chosen for the photodecomposition study because the absorption peak maximum of rhodamine B at 554 nm lies between the absorption band of these nanocrystals

SCHEME 2: Schematic Illustration of the Cu_2O Nanocrystal Formation Process[a]

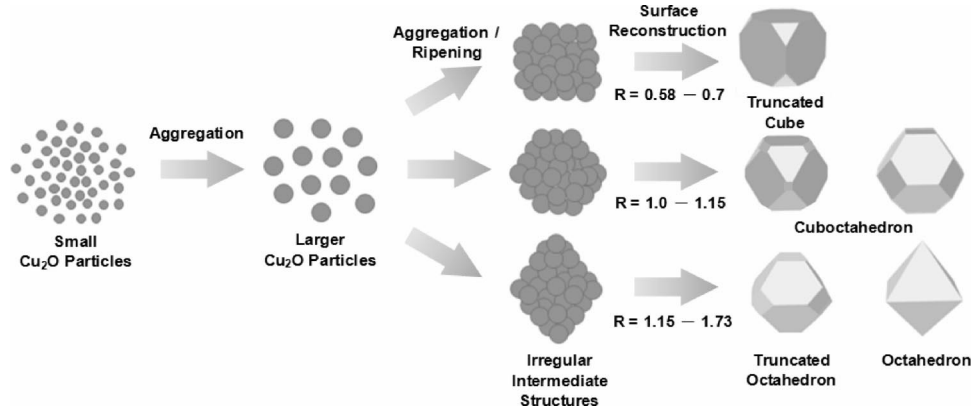

[a] *R* is the ratio of the growth rate along the [100] direction relative to that of the [111] direction.

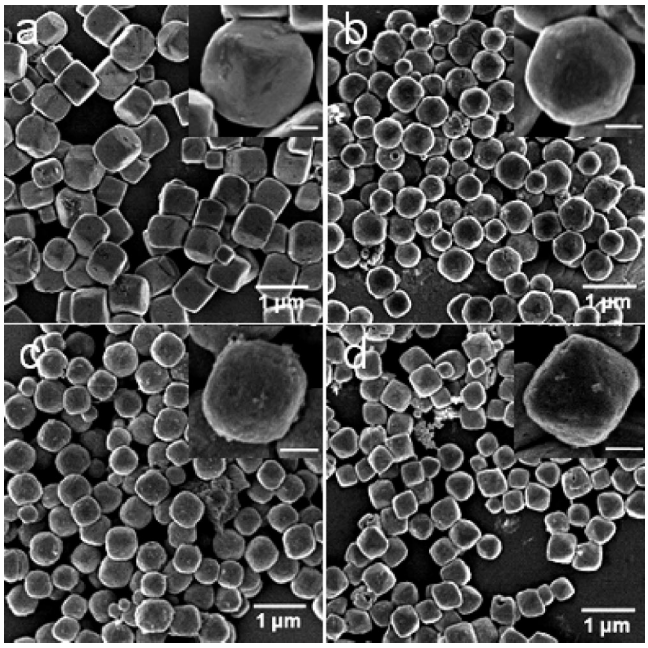

Figure 5. SEM images of the Cu_2O nanocrystals formed in sample bottles A–D by increasing the volume of NaOH added to the reaction mixture to 0.75 mL. The nanocrystal morphologies are the same as before with truncated cubic, cuboctahedral, truncated octahedral, and octahedral structures for the respective samples, but their average sizes have increased to (a) 532, (b) 565, (c) 467, and (d) 429 nm. The scale bars in all insets are equal to 200 nm.

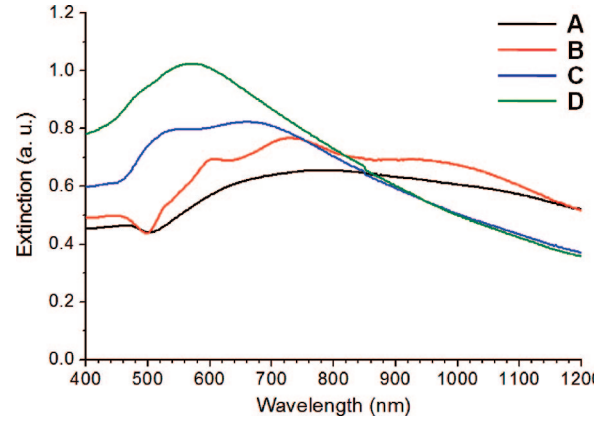

Figure 6. UV–vis absorption spectra of the Cu_2O nanocrystals in samples A–D.

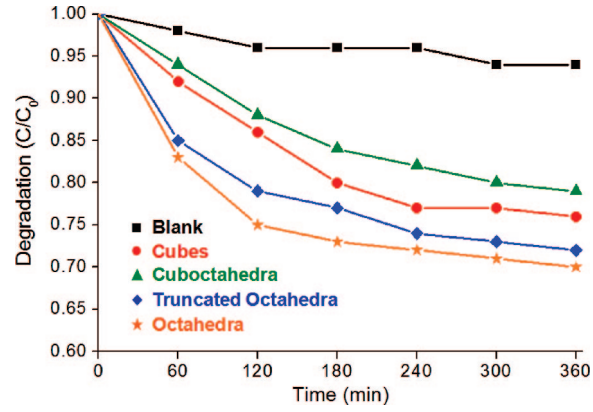

Figure 7. Extent of photodegradation of rhodamine B molecules (monitored at 554 nm) as a function of the irradiation time for the blank, truncated cubic, cuboctahedral, truncated octahedral, and octahedral nanocrystal samples. The blank sample did not contain any Cu_2O nanoparticles.

and their light scattering bands (see the Supporting Information). After irradiation for 6 h, the fraction of remaining absorption of rhodamine B was 0.94 for the blank sample, 0.79 for cuboctahedra, 0.76 for truncated nanocubes, 0.72 for truncated octahedra, and 0.70 for octahedra. This result suggests that octahedral Cu_2O nanoparticles with entirely {111} surfaces are more effective at photocatalysis reactions than nanoparticles of other shapes containing partial {100} and {110} surfaces. Similar observation has been made for Cu_2O nanocubes and octahedra with a smaller particle size of ~230 nm.[8] Truncated cubic nanocrystals showed a higher photodegradation extent than cuboctahedral particles presumably because their concentration in the solution is slightly greater, as revealed by their higher extinction values in the absorption spectrum (see the Supporting Information). The results serve as a rough comparison of the relative photocatalytic activities of the different crystal surfaces of Cu_2O, as accurate comparison of the total surface areas of the nanocrystals in the four solutions cannot be reliably obtained considering the uncertainty in the measurements of the quantity of the nanoparticles and their size distributions. Nevertheless, the comparison is still useful and insightful, as no such shape-controlled Cu_2O nanocrystals produced in a single system are available for comparison in other studies. The degradation rate gradually decreases partially because some nanocrystals adhered to the bottom and side walls of the quartz cells despite constant stirring of the solutions and fewer nanocrystals were being irradiated. Before irradiation, the solution volume in the quartz cell was 3.1 cm in height. After 6 h of irradiation, samples A, B, and C containing truncated cubic, cuboctahedral, and

truncated octahedral nanocrystals showed a slight drop in the solution volume to 2.8 cm in height. The volume change was not from thermal evaporation, as the cells were kept cool (the experiment was conducted in a cool air-conditioned environment at night, and the solution temperature was measured to be 19 and 23 °C before and after 1 h of irradiation). Remarkably, the solution volume for sample D with octahedral nanocrystals decreased significantly to just 1.8 cm in height. Visibly more gas bubbles were formed for this sample. The volume decrease may be due to a photoactivated splitting reaction of water to hydrogen and oxygen, as has been observed before.[6] If this is the case, it suggests that only octahedral Cu_2O nanocrystals are particularly effective for this reaction and that even truncated octahedral nanocrystals with largely {111} facets are not nearly capable of this important reaction. This insight points to the possibility of corners and facet edges of octahedral cuprous oxide nanocrystals as regions with higher catalytic activity. Interestingly, edges of triangular MoS_2 nanoplates have recently been demonstrated as the active sites for the electrochemical evolution of hydrogen gas.[28] Further study is necessary to verify the occurrence of this water-splitting reaction.

Conclusion

We have developed a simple and effective approach for the preparation of Cu_2O nanocrystals with systematic shape evolution. By simply varying the amount of hydroxylamine reductant added to the reaction mixture, monodisperse truncated cubic, cuboctahedral, truncated octahedral, and octahedral nanocrystals can be synthesized. Through an examination of the intermediate structures formed, a growth mechanism involving aggregation of seed particles, ripening, and surface reconstruction is proposed. SDS surfactant was found to be necessary for a precise control of these particle shapes. The sizes of these nanocrystals can be varied over a certain range by adjusting the amount of NaOH added. Optical characterization revealed their band gap energies and strong light scattering features. Octahedral nanocrystals with entirely {111} surfaces showed a better performance in the photocatalytic degradation of dye molecules than those of other shapes. These nanocrystals may find more applications in photocatalysis and organic synthesis. It is expected that these nanocrystals with different surfaces may exhibit different catalytic activities.

Acknowledgment. We thank the National Science Council of Taiwan for the support of this research (Grant NSC95-2113-M-007-031-MY3).

Supporting Information Available: Size distribution histograms, additional SEM images, plots of NaOH volume vs particle size and solution pH, photograph of the nanocrystal solutions, and additional UV−vis absorption spectra of the Cu_2O nanocrystals. This material is available free of charge via the Internet at http://pubs.acs.org.

References and Notes

(1) Ng, C. H. B.; Fan, W. Y. *J. Phys. Chem. B* **2006**, *110*, 20801.
(2) Zhang, J.; Liu, J.; Peng, Q.; Wang, X.; Li, Y. *Chem. Mater.* **2006**, *18*, 867.
(3) Zhang, H.; Zhu, Q.; Zhang, Y.; Wang, Y.; Zhao, L.; Yu, B. *Adv. Funct. Mater.* **2007**, *17*, 2766.
(4) Xu, H.; Wang, W.; Zhu, W. *J. Phys. Chem. B* **2006**, *110*, 13829.
(5) White, B.; Yin, M.; Hall, A.; Le, D.; Stolbov, S.; Rahman, T.; Turro, N.; O'Brien, S. *Nano Lett.* **2006**, *6*, 2095.
(6) Hara, M.; Kondo, T.; Komoda, M.; Ikeda, S.; Shinohara, K.; Tanaka, A.; Kondo, J. N.; Domen, K. *Chem. Commun.* **1998**, 357.
(7) Tang, B.-X.; Wang, F.; Li, J.-H.; Xie, Y.-X.; Zhang, M.-B. *J. Org. Chem.* **2007**, *72*, 6294.
(8) Kuo, C.-H.; Chen, C.-H.; Huang, M. H. *Adv. Funct. Mater.* **2007**, *17*, 3773.
(9) Gou, L.; Murphy, C. J. *Nano Lett.* **2003**, *3*, 231.
(10) Gou, L.; Murphy, C. J. *J. Mater. Chem.* **2004**, *14*, 735.
(11) Wang, D.; Mo, M.; Yu, D.; Xu, L.; Li, F.; Qian, Y. *Cryst. Growth Des.* **2003**, *3*, 717.
(12) Siegfried, M. J.; Choi, K.-S. *J. Am. Chem. Soc.* **2006**, *128*, 10356.
(13) Siegfried, M. J.; Choi, K.-S. *Adv. Mater.* **2004**, *16*, 1743.
(14) Li, H.; Liu, R.; Zhao, R.; Zheng, Y.; Chen, W.; Xu, Z. *Cryst. Growth Des.* **2006**, *6*, 2795.
(15) Lu, C.; Qi, L.; Yang, J.; Wang, X.; Zhang, D.; Xie, J.; Ma, J. *Adv. Mater.* **2005**, *17*, 2562.
(16) Jiao, S.; Xu, L.; Jiang, K.; Xu, D. *Adv. Mater.* **2006**, *18*, 1174.
(17) Teo, J. J.; Chang, Y.; Zeng, H. C. *Langmuir* **2006**, *22*, 7369.
(18) Chang, Y.; Teo, J. J.; Zeng, H. C. *Langmuir* **2005**, *21*, 1074.
(19) Wang, Z.; Chen, X.; Liu, J.; Mo, M.; Yang, L.; Qian, Y. *Solid State Commun.* **2004**, *130*, 585.
(20) Xu, H.; Wang, W. *Angew. Chem., Int. Ed.* **2007**, *46*, 1489.
(21) Singh, D. P.; Neti, N. R.; Sinha, A. S. K.; Srivastava, O. N. *J. Phys. Chem. C* **2007**, *111*, 1638.
(22) Wang, W.; Wang, G.; Wang, X.; Zhan, Y.; Liu, Y.; Zheng, C. *Adv. Mater.* **2002**, *14*, 67.
(23) Tan, Y.; Xue, X.; Peng, Q.; Zhao, H.; Wang, T.; Li, Y. *Nano Lett.* **2007**, *7*, 3723.
(24) Siegfried, M. J.; Choi, K.-S. *Angew. Chem., Int. Ed.* **2005**, *44*, 3218.
(25) Chang, Y.; Zeng, H. C. *Cryst. Growth Des.* **2004**, *4*, 273.
(26) Seo, D.; Park, J. C.; Song, H. *J. Am. Chem. Soc.* **2006**, *128*, 14863.
(27) Wang, Z. L. *J. Phys. Chem. B* **2000**, *104*, 1153.
(28) Jaramillo, T. F.; Jørgensen, K. P.; Bonde, J.; Nielsen, J. H.; Horch, S.; Chorkendorff, I. *Science* **2007**, *317*, 100.

JP8060027